Redox Biology 24 (2019) 101184

Contents lists available at ScienceDirect

Redox Biology

journal homepage: www.elsevier.com/locate/redox

Research Paper

FoxO6-mediated IL-1β induces hepatic insulin resistance and age-related inflammation *via* the TF/PAR2 pathway in aging and diabetic mice

Dae Hyun Kim[a], Bonggi Lee[b], Jaewon Lee[a], Mi Eun Kim[c], Jun Sik Lee[c], Jae Heun Chung[d], Byung Pal Yu[e], H. Henry Dong[f], Hae Young Chung[a,*]

[a] Department of Pharmacy, College of Pharmacy, Pusan National University, 2, Busandaehak-ro 63beon-gi, Geumjeong-Gu, Busan, 46241, South Korea
[b] Korean Medicine (KM)-Application Center, Korea Institute of Oriental Medicine (KIOM), Daegu, 41062, Republic of Korea
[c] Department of Biology, College of Natural Science, Chosun University, Gwangju, 501-759, Republic of Korea
[d] Department of Internal Medicine, Pusan National University Yangsan Hospital, Yangsan, 50612, South Korea
[e] Department of Physiology, The University of Texas Health Science Center at San Antonio, TX, 78229, USA
[f] Department of Pediatrics, Children's Hospital of Pittsburgh of UPMC, School of Medicine, University of Pittsburgh, Pittsburgh, PA, 15224, USA

ARTICLE INFO

Keywords:
FoxO6
IL-1β
TF/PAR2 signaling
Aging
Inflammation
Insulin resistance

ABSTRACT

FoxO has been proposed to play a role in the promotion of insulin resistance, and inflammation. FoxO is a pro-inflammatory transcription factor that is a key mediator of generation of inflammatory cytokines such as IL-1β in the liver. However, the detailed association of FoxO6 with insulin resistance and age-related inflammation has not been fully documented. Here, we showed that FoxO6 was elevated in the livers of aging rats and obese mice that exhibited insulin resistance. In addition, virus-mediated FoxO6 activation led to insulin resistance in mice with a notable increase in PAR2 and inflammatory signaling in the liver. On the other hand, FoxO6-KO mice showed reduced PAR2 signaling with a decrease in inflammatory cytokine expression and elevated insulin signaling. Because FoxO6 is closely associated with abnormal production of IL-1β in the liver, we focused on the FoxO6/IL-1β/PAR2 axis to further examine mechanisms underlying FoxO6-mediated insulin resistance and inflammation in the liver. In vitro experiments showed that FoxO6 directly binds to and elevates IL-1β expression. In turn, IL-1β treatment elevated the protein levels of PAR2 with a significant decrease in hepatic insulin signaling, whereas PAR2-siRNA treatment abolished these effects. However, PAR2-siRNA treatment had no effect on IL-1β expression induced by FoxO6, indicating that IL-1β may not be downstream of PAR2. Taken together, we assume that FoxO6-mediated IL-1β is involved in hepatic inflammation and insulin resistance via TF/PAR2 pathway in the liver.

1. Introduction

Forkhead transcription factor (FoxO) plays key roles in the induction of various downstream genes involved in the inhibition of cellular metabolism, cell cycle, cell death, and oxidative stress responses [1]. Furthermore, it has been reported that FoxO family members are associated with insulin resistance partially by suppressing the downstream pathways of the PI3K/Akt signaling [2]. The roles of FoxO1 in glucose metabolism was extensively studied. A FoxO1 gain-of-function mutant mice showed a diabetic phenotype in part by the suppression of genes related to insulin sensitivity in the liver, adipocytes, and pancreatic β cells [3]. FoxO1 also induced insulin resistance and inflammation and stimulated the production of inflammatory cytokines including IL-1β in macrophages [4]. However, the roles of FoxO6 in inflammatory signaling including IL-1β production have not been fully understood.

Low-grade, chronic inflammation, and insulin resistance are two key processes that operate interdependently during aging and in type 2 diabetes (T2D). The former is accompanied by the elevated production of pro-inflammatory cytokines in the body, whereas the latter is characterized by significantly diminished responsiveness of peripheral tissues to normal plasma insulin levels. Although there is a lack of consensus regarding the cause-and-effect relationship between chronic exposure to low-grade inflammation and the onset of insulin resistance, these two physio-pathological traits share mechanisms of cross-talk that integrate abnormal production of inflammatory cytokines with the development of insulin resistance in T2D [5]. To delineate the mechanisms linking inflammation and insulin resistance, in the present

* Corresponding author. College of Pharmacy, Pusan National University, Pusan National University, 2, Busandaehak-ro 63beon-gi, Geumjeong-Gu, Busan, 46241, South Korea.
E-mail addresses: hyjung@pusan.ac.kr, mrca@pusan.ac.kr (H.Y. Chung).

https://doi.org/10.1016/j.redox.2019.101184
Received 2 December 2018; Received in revised form 18 March 2019; Accepted 28 March 2019
Available online 03 April 2019

study, we set out to investigate their relationship by defining the novel role of FoxO6 in protease-activated receptor-2 (PAR2)/Tissue factor (TF) signaling.

PAR2 is a G protein-coupled receptor that has been shown to play an important role in mesenchymal cell activation and inflammatory signaling [6]. The PAR2 signaling has been associated with various signaling cascade. The PAR2-activating tissue factor VIIa can also activate inflammation in adipose tissue through the production of TNF-α and IL-6 and cause insulin resistance through the suppression of Akt phosphorylation [7], and monocyte recruitment [8]. The confluence of these PAR2 proteases during tissue injury and remodeling leads to a microenvironment that may trigger prolonged pathological activation of the PAR2 signaling pathway. Included is the activation of mitogen-activated protein kinases (ERK, p38, and JNK) involved in proliferation, inflammation, and differentiation of mesenchymal cells *via* the TGF-β, TNF-α, IL-1β, and NF-κB pathways during tissue fibrosis [9,10]. Nevertheless, it is unclear whether FoxO6 is associated with PAR2 signaling in the liver.

Aging represents the functional deficits accumulated in the organism over time. The aging process is accompanied with many age-related chronic diseases such as diabetes, cancer, arthritis, dementia, vascular diseases, obesity, and metabolic syndrome [11]. It is now well established that increased incidences of diabetes and obesity are closely associated with insulin resistance [12]. Solar lentigines are macular hyperpigmented lesions associated with sun exposure, inflammation, and age through PAR2 [13]. Age-related changes in vascular PAR2 and increased oxidative stress in metabolic syndrome [14]. Uncontrolled regulation of insulin signaling in inflammatory status causes T2D and accelerates the aging process. However, very little is known about the roles of PAR2 in the liver under diabetic and aging conditions.

In the present study, we explored interplay among FoxO6, IL-1β, and PAR2 for insulin resistance and inflammation in the liver.

We specifically focused on whether the FoxO6 activates PAR2 through IL-1β and studied its effects on glucose metabolism and inflammation.

2. Material and methods

2.1. Animals

C57BL/6J mice aged 6 weeks were purchased from the Jackson Laboratory. The mice received standard rodent chow and water *ad libitum*, and were kept in sterile cages with a 12 h light/dark cycle. The C57BL/6J mice were classified by body weight and randomly assigned to two groups; the mice in one group received an intravenous injection of an adenoviral vector containing a constitutively active FoxO6 allele (AdV-FoxO6-CA) in the tail, whereas the mice in the other group received an intravenous injection of an AdV-null vector in the tail, both at 1.5×10^{11} plaque forming units (pfu)/kg body weight. The mice were sacrificed two weeks after the AdV-FoxO6-CA injection. The mice fasted for 24 h, and venous blood samples were collected from the tail in order to determine blood glucose levels, as previously described.

Specific pathogen-free male Fischer 344 rats (6 or 24 months old) were obtained from Samtako (Osan, Korea) and fed a diet with the following composition: 21% soybean protein, 15% sucrose, 43.65% dextrin, 10% corn oil, 0.15% α-methionine, 0.2% choline chloride, 5% salt mix, 2% vitamin mix, and 3% Solka-Floc fiber. Eight-week-old male C57BLKS/J-lean and C57BLKS/J-db/db (diabetic) mice were purchased from Japan SLC. The mice were maintained under a 12 h light/dark cycle at 23 ± 1 °C and 50 ± 5% relative humidity under specific pathogen-free conditions. Homozygote PAR2 knockout mice ($PAR2^{-/-}$; strain: B6.Cg-*F2rl1*^{tm1Mslb}/J) aged 8 weeks were obtained from Dr. Yu (Pusan National University, Busan, Korea). The livers from FoxO6-Tg and FoxO6-KO mice were obtained from the University of Pittsburgh Medical Center, Pittsburgh, PA, USA.

The animal protocol used in this study was reviewed and approved by the Pusan National University Institutional Animal Care and Use Committee (PNU-IACUC) with respect to ethics and animal care.

2.2. Cell culture system

HepG2 cells (human hepatocellular carcinoma) were obtained from the American Type Culture Collection (ATCC, Rockville, MD, USA). Cells were cultured in Dulbecco's Modified Eagle Medium (DMEM) (Nissui Co., Tokyo) supplemented with 10% heat-inactivated (56 °C for 30 min) fetal bovine serum (Gibco, Grand Island, NY), 233.6 mg/ml glutamine, 100 mg/mL penicillin streptomycin, and 0.25 μg/mL amphotericin B. Cells were maintained at 37 °C in a humidified 5% CO_2/95% air atmosphere.

2.3. Materials

Western blotting reagents were purchased from Amersham (Bucks, UK). RNAzol™ B was obtained from TEL-TEST, Inc. (Friendwood, TX, USA). Antibodies against β-actin, Histone H1, p-IRS (ser), p-IRS (tyr), p-Akt, total-Akt, p-c-Jun, C-Jun, and COX-2 were obtained from Santa Cruz Biotechnology (Santa Cruz, CA, USA). Antibodies against FoxO6 and p-FoxO6 (Ser184) were obtained from Dr. H. H. Dong (University of Pittsburgh, PA). Anti-rabbit IgG-horseradish peroxidase-conjugated antibody and anti-mouse IgG-horseradish peroxidase-conjugated antibody were obtained from Amersham (Bucks, UK). Horseradish peroxidase-conjugated donkey anti-sheep/goat IgG was purchased from Serotec (Oxford, UK). Polyvinylidene difluoride (PVDF) membranes were obtained from the Millipore Corporation (Bedford, MA, USA).

2.4. Nuclear extract preparation

Frozen rat liver tissues (20–40 mg) were rinsed in PBS buffer and then transferred to a Dounce tissue grinder (Wheaton Manufacturers, NJ). Solution A (10 mM HEPES pH 7.9, 10 mM KCl, 0.1 mM EDTA, 0.1 mM EGTA, 1 mM DTT, 0.5 mM PMSF) was then added to the tissues (2.5 g/ml). Tissues were homogenized with five strokes of a pestle and after adding NP-40 (0.5%), then further homogenized with an additional five strokes. Homogenates were transferred to Eppendorf tubes and centrifuged in a microcentrifuge (Beckman) for 5 min at 12000 rpm.

Supernatants contained predominantly cytoplasmic constituents. To obtain nuclear pellets, 400 μl of solution C (20 mM HEPES pH 7.9, 0.4 M NaCl, 1 mM of each of EDTA, EGTA, DTT, and PMSF) was added to supernatants. Tubes were mixed thoroughly and placed on a small rotatory shaker for 15 min. Finally, they were centrifuged at 12000 rpm for 10 min in a microcentrifuge. Supernatants, which contained nuclear proteins, were then removed, transferred carefully to fresh tubes, and stored at −80 °C until required for Western blotting. Protein contents were determined using the Bicinchoninic Acid Protein Assay (Sigma).

2.5. Western blotting

Homogenized samples were boiled for 5 min with gel-loading buffer (125 mM Tris-Cl, 4% SDS, 10% 2-mercaptoethanol, pH 6.8, 0.2% bromophenol blue) at a ratio of 1:1. Equal amounts of protein were separated by sodium dodecyl sulfate-polyacrylamide gel electrophoresis, using 6–17% gels and then transferred to PVDF membranes at 15 V for 1 h using a semi-dry transfer system. Membranes were then immediately placed into a blocking buffer 10 mM Tris (pH 7.5), 100 mM NaCl, and 0.1% Tween-20 containing 1% non-fat milk. Blots were blocked at room temperature for 1 h, and membranes were incubated with the appropriate specific primary antibody at 25 °C for 1 h, followed by horseradish peroxidase-conjugated secondary antibody at 25 °C for 1 h. Antibody labeling was detected using enhanced chemiluminescence, according to the manufacturer's instructions. Molecular weights were determined using pre-stained protein markers.

2.6. Transfection and luciferase reporter assay

IL-1β activities were estimated using an IL-1β-luciferase vector (Dr. Dong, University of Pittsburgh, PA, USA) that contained a specific binding sequence for FoxO6. Transfection was carried out using Lipofectamine 2000 (Invitrogen). Briefly, 1×10^4 cells per well were seeded in 48-well plates. When the cultured cells reached approximately 40% confluence, they were treated with DNA/Lipofectamine 2000 complexes (1 μg/μl) in 500 μl normal media (with 10% serum) for 24 h, then treated with the vector containing FoxO6 (100 MOI) at 24 h after transfection. Then, the cells were washed with PBS and subjected to the Steady-Glo Luciferase Assay System (Promega, Madison, WI, USA). Luciferase activity was measured by a luminometer (GENious, TECAN, Salzburg, Austria).

2.7. Small interfering RNA-mediated gene silencing

To knock down PAR2 in HepG2 cells, we utilized scrambled or PAR2-siRNAs obtained from a commercial source (IDT, Coralville, Iowa, USA). Transfection was carried out using the Lipofectamine 2000 reagent (Invitrogen, Grand Island, New York, USA). The cells were treated with scrambled or PAR2-siRNA-Lipofectamine complexes (20 nM) in Opti-MEM (Invitrogen) without serum. After incubation for 4 h, the transfection medium was replaced with fresh medium, and the cells were incubated for another 24 h, during which they were treated with an adenoviral vector containing FoxO6 at the indicated times.

2.8. Serum biochemical analysis and cytokine measurements

Serum glucose was analyzed using kits from Bioassay Systems (Hayward, CA, USA). Specific kits were used, following the manufacturer's instructions, to determine the concentrations of insulin (Shibayagi, Japan). Cytokine levels were measured using the Luminex multiplex analysis system (Millipore, Billerica, MA, USA).

2.9. Glucose tolerance test

Mice were fasted for 24 h, followed by intraperitoneal injection of glucose (2 g/kg). Blood glucose levels were measured before and after the glucose injection by using a Glucometer Elite meter (Bayer, IN, USA).

2.10. RNA isolation and real-time RT-PCR

RNA isolation from liver (20 mg) cells and HepG2 cells (approximately 2×10^6 cells) was performed using the RNeasy Mini Kit (Qiagen, Valencia, CA, USA). Real-Time Quantitative Reverse Transcription PCR (qRT-PCR) with SYBR Green was used for quantifying mRNA concentrations in a CFX Connect System (Bio-Rad Laboratories Inc., Hercules, CA, USA). All primers were obtained from Integrated DNA Technologies (Coralville, IA, USA).

2.11. Chromatin immunoprecipitation (ChIP) assay

ChIP was used to study the interaction between FoxO6 and the IL-1β promoter DNA. HepG2 cells (2×10^5 cells) were transfected with pGH11 in the presence of the FoxO6 vector at a multiplicity of infection (MOI) of 100 pfu/cell in triplicate. After a 24-h incubation period, the cells were subjected to a ChIP assay using the anti-FoxO6 antibody and the ChIP assay kit (Upstate Biotechnology). The immunoprecipitates were analyzed by immunoblot assays using rabbit anti-FoxO6 antibody, and by PCR assay to detect coimmunoprecipitated DNA using IL-1β promoter-specific primers (forward 5′-TCTATTTCCCTTCAGTGCTG-3′, reverse 5′-TTCATGAGCACAGTCCATCT-3′), which flank the consensus FoxO6 binding site in the human IL-1β promoters, respectively.

2.12. Immunoprecipitation (IP) of nuclear extracts

Nuclear extracts were immunoprecipitated in a buffer containing 40 mM Tris-HCl (pH 7.6), 120 mM NaCl, 20 mM β-glycerophosphate, 20 mM NaF, 2 mM sodium orthovanadate, 5 mM EDTA, 1 mM PMSF, 0.1% NP40, leupeptin (2 μg/ml), aprotinin (1 μg/ml), and pepstatin A (1 μg/ml). Aliquots of nuclear extracts were than precleared using a 50% protein A agarose for 30 min at 4 °C, centrifuged at 12,000 × *g* at 4 °C for 15 min, incubated overnight at 4 °C with the required antibody, and then incubated overnight at 4 °C with 50% protein A agarose slurry. After washing immunoprecipitates three times with IP buffer, immunoprecipitated proteins were analyzed by SDS-PAGE, and Western blotting analysis was performed as described above.

2.13. Immunohistochemistry

For immunostaining, liver sections were treated with 0.6% H_2O_2 in Tris-buffered saline (TBS; pH7.5) to block endogenous peroxidase for 15 min at RT. After incubation, sections were incubated with TBS containing 0.1% Triton X-100 and 3% goat serum (TBS-TS) at 37 °C for 1 h and then incubated with primary anti-F4/80 or anti-CD68 antibody (Santa Cruz, Texas, USA) in TBS-TS overnight at 4 °C. Sections were then further incubated with secondary goat anti-mouse IgG-HRP antibody (Santa Cruz) at RT for 3 h. Sections were then stained with diaminobenzidine (DAB) solution and mounted with Dako mounting medium (Dako, Glostrup, Denmark), and cover slipped. Images were acquired using an Olympus IX71 microscope (Olympus, Tokyo, Japan).

2.14. Flow cytometric analysis

HepG2 cells were transfected with PAR2 siRNA by Lipofectamine 2000. siRNA and Lipofectamine 2000 were mixed and incubated at room temperature for 20 min. The medium was replaced with serum-free media, and then the siRNA mixture was added to the cells for 4 h. After incubation, the medium was replaced with complete cell culture medium and the cells were cultured for 20 h. After which, cells were treated with 10 ng/ml IL-1β peptide for 24 h. The cells were collected in conical tubes and washed 2 times with cold PBS. IL-1β intracellular staining was performed with BD cytofix/cytoperm Fixation/Permeabilization Solution Kit (BD Biosciences, NJ, USA). The cells were incubated with 250 μl BD Cytofix/Cytoperm solution per tube for 20 min at 4 °C and then the cells were washed 2 times with BD Perm/Wash™ buffer. Diluted FoxO6 antibody (1:500 dilution) was added into cells and incubated at 4 °C for 30 min. After incubation, the cells were washed 2 times with BD Perm/Wash™ buffer and then treated with FITC-conjugated rabbit IgG antibody (1:500) at 4 °C for 30 min in the dark room. The cells were fixed with 4% paraformaldehyde following washing with BD Perm/Wash™ buffer and analyzed by flow cytometry (FC500, Beckman Coulter, CA, USA).

2.15. Statistical analysis

ANOVA was conducted to determine the significance of differences between groups. Fisher's Protected LSD post-hoc test was used to determine the significance of differences between group means. P-values < 0.05 were taken to indicate statistical significance.

3. Results

3.1. FoxO6 induces insulin resistance and cytokines in the FoxO6-overexpressed liver

We investigated the effect of FoxO6 in mice injected with a viral vector containing FoxO6. We generated mice expressing constitutively active FoxO6-CA in the liver. Male mice injected with FoxO6-CA developed hyperinsulinemia, culminating in significantly elevated fasting

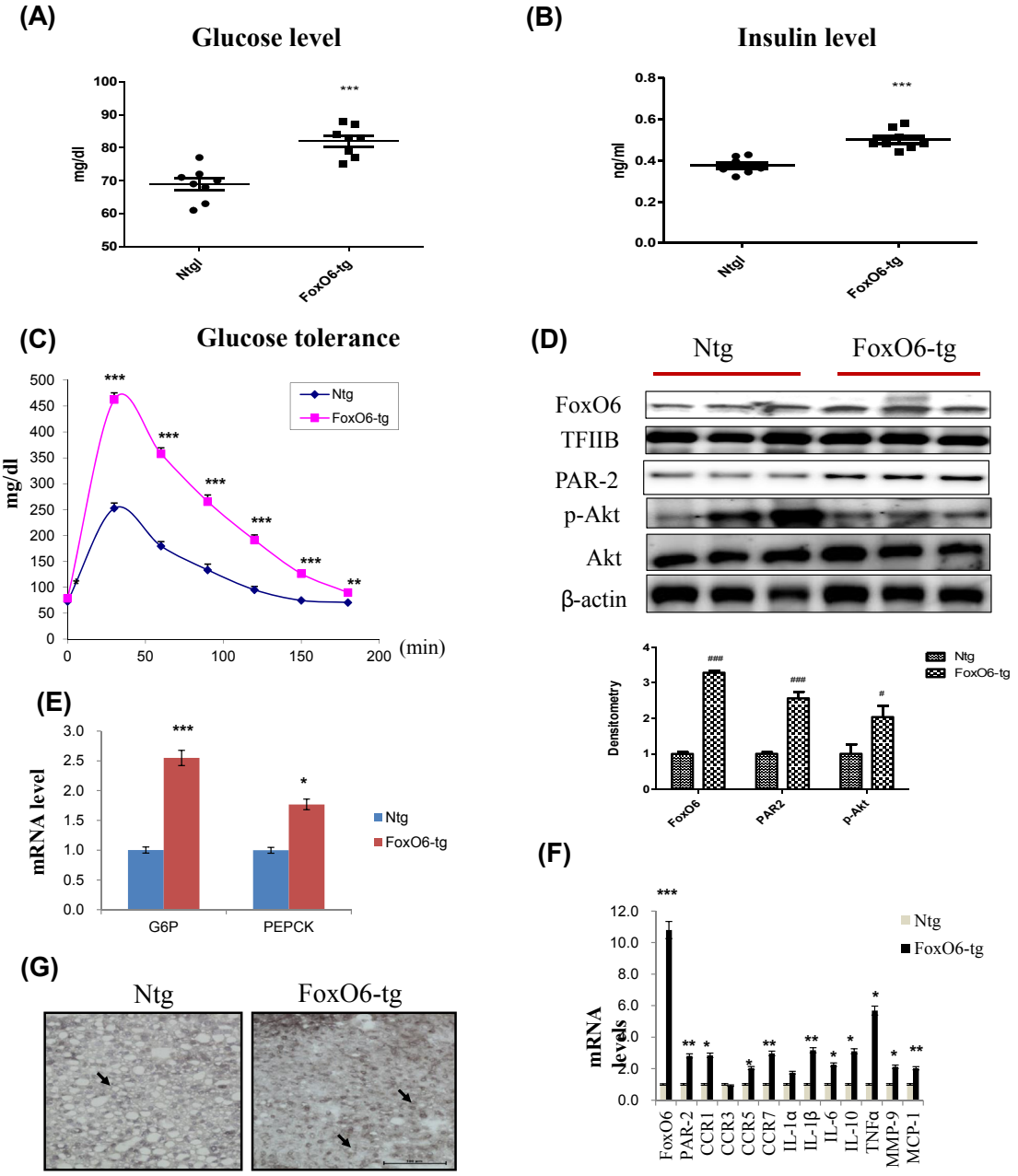

Fig. 1. FoxO6 overexpression induced insulin resistance and cytokine production. Serum levels of pro-cytokines in mice injected with either FoxO6-CA or null adenoviral vectors, assessed over a period of 13 days (n = 6 in each group): (A) Glucose level (B) Insulin level (C) Glucose tolerance test in the serum of FoxO6-CA. (D) FoxO6, PAR2, p-Akt, and total-Akt levels were assessed using nuclear and cytosolic proteins in FoxO6-Tg mice. TFIIB is the loading control of the nuclear fraction. β-actin is the loading control of the cytosolic fractions. Results are representative of three independent experiments. Bars in densitometry data represent means ± SE, and significance was determined using an unpaired *t*-test: $^{\#}p < 0.05$, $^{\#\#\#}p < 0.001$ vs. Ntg. (E) G6Pase and PEPCK mRNA levels of gluconeogenesis genes in FoxO6-tg liver. $^{*}p < 0.05$, $^{***}p < 0.001$ vs. Ntg. (F) The expression of relevant genes (FoxO6, PAR2, CCR1, CCR3, CCR5, CCR7, IL-1α, IL-1β, IL-6, IL-10, TNFα, MMP-9, and MCP-1) was analyzed by qPCR. The results were normalized with respect to actin levels. Real-time PCR analyses were performed to determine mRNA levels in liver tissues of FoxO6-Tg mice. $^{*}p < 0.05$, $^{**}p < 0.01$, $^{***}p < 0.001$ vs. Ntg. (G) Macrophage infiltration was observed in the liver tissue of mice. F4/80 was used to identify macrophages, which can be seen as cells stained dark grey (marked with an arrow) in FoxO6-Tg and Ntg (×20).

glucose levels (Fig. 1A), insulin levels (Fig. 1B), and glucose intolerance (Fig. 1C), compared to age/sex-matched control littermates.

To determine whether FoxO6 plays a role in linking insulin resistance to aberrant cytokine expression, we studied insulin resistance and cytokine expression in FoxO6-Tg mice. FoxO6 resulted in significantly increased expression of FoxO6 and PAR2 in the liver of FoxO6-Tg mice (Fig. 1D). Also, the increased FoxO6 expression was associated with the increased expression of PEPCK and G6Pase, two key genes in gluconeogenesis (Fig. 1E). However, this effect was accompanied by increased expression of the cytokines TNFα, IL-6, IL-1β, and MCP-1. FoxO6 overexpression resulted in a significant increase in CCR1, CR5, CCR7, IL-1β, IL-6, IL-10, TNFα, and MMP-9 production, without altering the production of other cytokines such as CCR3 or IL-1α (Fig. 1F). These data indicate the important roles of FoxO6 in regulating cytokine production *in vivo*. Because of the close association of FoxO6 with abnormal production of IL-1β in the liver, we focused on delineation of the molecular basis underlying FoxO6-mediated induction of cytokines.

Inflammatory pathways play an important role in impaired glucose metabolism and insulin production. Moreover, the inflammatory

response was assumed to be the consequence rather than the cause of the disease. Liver inflammation is characterized by infiltration and expansion of macrophages [15]. To examine whether FoxO6 induced macrophage infiltration in FoxO6-Tg, we performed histologic analysis of liver tissue in the Non-transgenic (Ntg) group compared with the FoxO6-Tg group. As shown in Fig. 1G, macrophage infiltration was substantially higher in FoxO6-Tg than in Ntg. Deletion of FoxO6 inhibited macrophage infiltration (Supplementary Fig. 1). We next evaluated the expression levels of pro-inflammatory cytokines and chemokines in the FoxO6-Tg group and found that pro-inflammatory cytokines and chemokines were significantly induced. These results indicate that FoxO6-Tg strongly induces macrophage infiltration and pro-inflammatory cytokines as well as chemokines.

3.2. Interaction of TF and PAR2 in the FoxO6-Tg liver

The liver and other tissues contain PAR2, a G-protein coupled receptor that has been shown to play an important role in inflammation and steatosis [16]. Four forms of PARs have been reported (PAR-1 through PAR-4). In particular, PAR2 is activated by trypsin-like proteases, such as tryptase, and by coagulation factors VIIα and Xα when TF expression.

PAR2 mRNA levels increased about 3-fold and PAR1 level increased 2-fold in the FoxO6-Tg liver. No other significant differences in hepatic PAR3 and PAR4 mRNA levels were detected in FoxO6-Tg (Fig. 2A). However, mRNA levels of TF significantly increased in the FoxO6-Tg liver (Fig. 2B). In the immunoprecipitation study, TF and PAR2 were observed to interact in FoxO6-Tg (Fig. 2C).

3.3. Deletion of FoxO6 suppresses various cytokines in the FoxO6-KO liver

FoxO6-KO mice were viable and exhibited significantly lower fasting blood glucose levels than WT control mice. In the glucose tolerance tests, FoxO6-KO mice exhibited significantly improved blood glucose profiles [17]. To determine the effect of FoxO6 depletion on systemic inflammation, we measured cytokine levels. Significant differences in pro-inflammatory cytokines levels were detectable between FoxO6-KO and WT littermates (n = 6/group). We also measured PAR2 and insulin signaling by western blotting. PAR2, FoxO6, AP-1, and JNK signaling were suppressed in the FoxO6-KO group (Fig. 3A). However, IRS/Akt signaling increased in the FoxO6-KO liver. Fig. 3B shows qRT-PCR results for the FoxO6-KO liver. FoxO6 had an enhanced stimulatory effect on cytokine expression. This effect was accompanied by decreased mRNA levels of TNFα, IL-1β, and MCP-1 (Fig. 3B). However, FoxO6 and PAR2 levels were also suppressed in FoxO6-KO mice. In terms of glucose metabolism, FoxO6-KO suppressed the expression of G6Pase and PEPCK, two key genes in gluconeogenesis (Supplementary Fig. 2).

3.4. FoxO6-induced IL-1β regulates insulin signaling and inflammation through PAR2 in HepG2 cells

We examined PAR2 expression in HepG2 cells exposed to FoxO6-virus. Cells were treated with or without different concentrations of FoxO6-carrying viruses (50–200 MOI). Treatment with 50–200 MOI of FoxO6 increased the protein level of PAR2 (Supplementary Fig. 3). Considering the decrease and increase in PAR2 protein levels in FoxO6 deficient and activated conditions, respectively, FoxO6 may regulate PAR2 expression. To examine the hypothesis that FoxO6 targets the IL-1β gene for transactivation, we investigated whether FoxO6 stimulated IL-1β expression in HepG2 cells. FoxO6 bound to the IL-1β promoter, as determined by luciferase assay (Fig. 4A) and a chromatin immunoprecipitation assay (Fig. 4B), performed in HepG2 cells transfected with empty and FoxO6-containing vectors. FoxO6 was associated

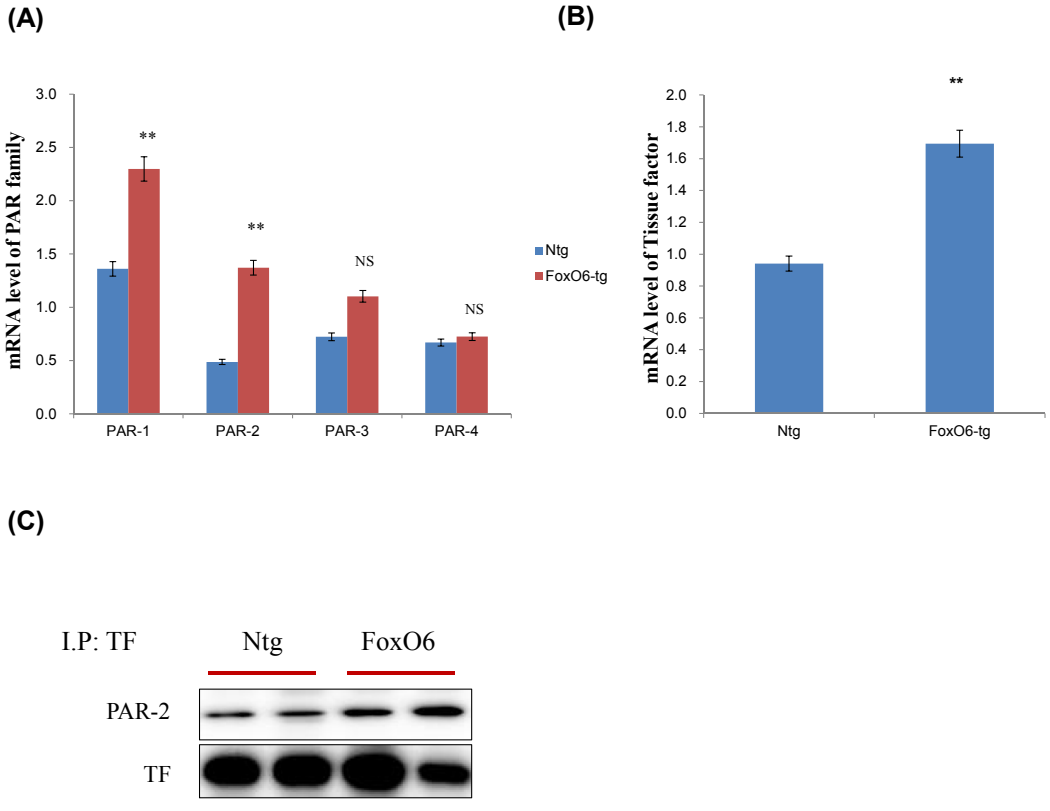

Fig. 2. The interaction between tissue factor and PAR2 in FoxO6-Tg liver. (A) PAR1, PAR2, PAR3, and PAR4 mRNA in FoxO6-Tg liver. Real-time PCR analyses were performed to determine mRNA levels in liver tissues. $^{**}p < 0.01$ vs. Ntg. (B) Tissue factor (TF) mRNA level in FoxO6-Tg liver. $^{**}p < 0.01$ vs. Ntg. (C) Cytosolic extracts were prepared from the liver of FoxO6-Tg mice. Immunoprecipitated TF was determined to be physically associated with PAR2 by Western blotting.

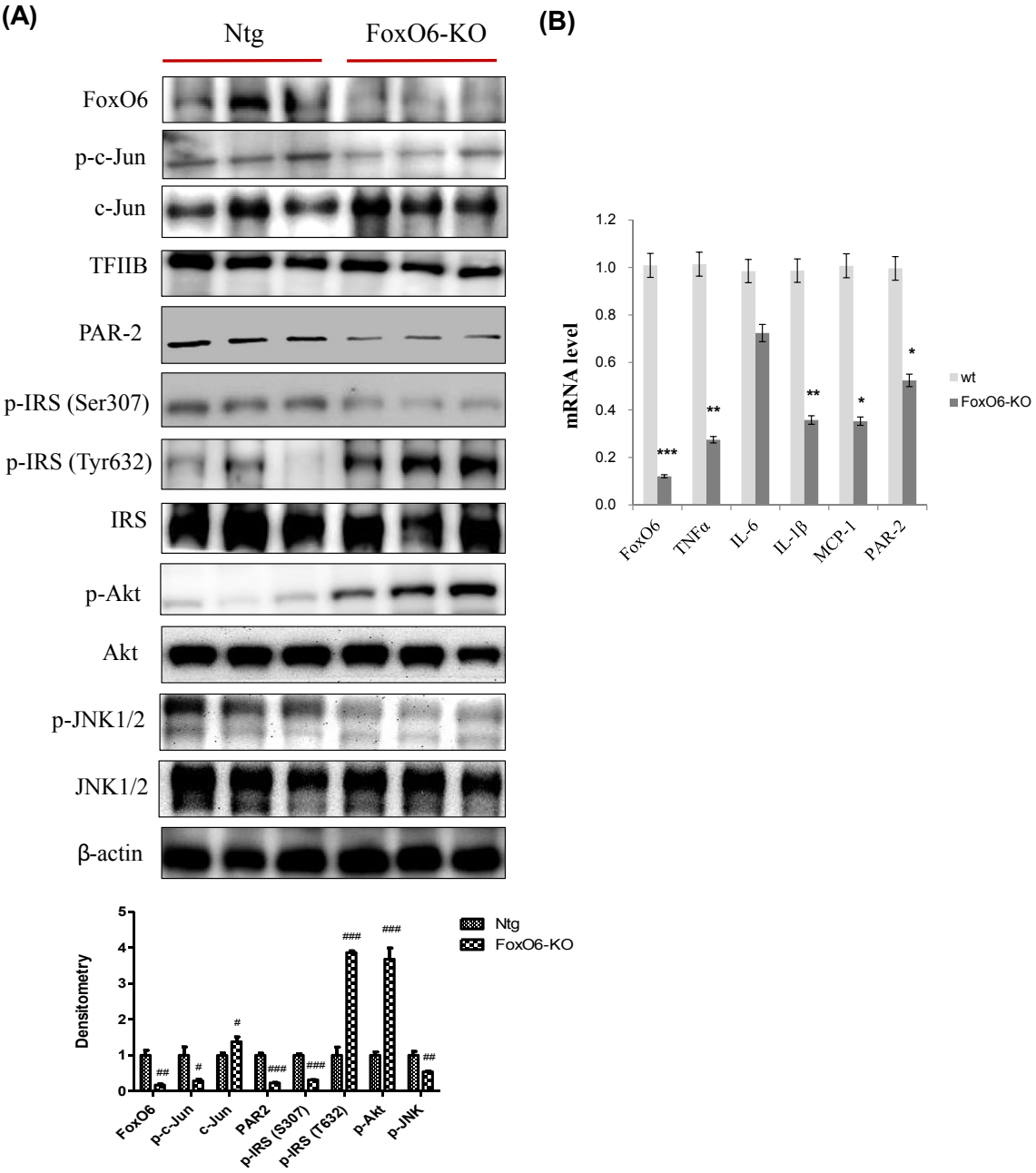

Fig. 3. Deletion of FoxO6 suppresses various cytokines. (A) FoxO6, p-c-Jun, c-Jun, PAR2, p-IRS (S307), p-IRS (T632), IRS, p-Akt, Akt, p-JNK1/2, and JNK1/2 levels were assessed using nuclear and cytosolic proteins from FoxO6-KO mice. TFIIB was the loading control of the nuclear fraction. β-actin was the loading control of the cytosolic fractions. Results are representative of three independent experiments. Bars in densitometry data represent means ± SE, and significance was determined using an unpaired *t*-test: $^{\#}p < 0.05$, $^{\#\#}p < 0.01$, $^{\#\#\#}p < 0.001$ vs. Ntg. (B) FoxO6, TNFα, IL-6, IL-1β, MCP-1, and PAR2 mRNA. Real-time PCR analyses were performed to determine mRNA levels in liver tissues of FoxO6-knockout mice. $^{*}p < 0.05$, $^{**}p < 0.01$, $^{***}p < 0.001$ vs. wt.

with IL-1β promoter DNA in cells transfected with FoxO6 and exhibited a stimulatory effect on IL-1β expression compared with the empty vector in HepG2 cells. Constitutively active FoxO6-CA treatment significantly increased the phosphorylation of c-Jun, a major component of the pro-inflammatory transcription factor AP-1 in the nucleus of the liver cells, indicating that AP-1 may be activated by FoxO6 (Fig. 4C).

In addition, cells treated with FoxO6-CA showed increased the protein levels of TF, PAR2, and IL-1β and elevated the phosphorylation of ERK and JNK proteins (Fig. 4D). This effect was accompanied by increased mRNA levels of FoxO6, IL-1β, G6Pase, and PEPCK (Fig. 4E).

3.5. Deletion of PAR2 suppresses insulin resistance and inflammation in vitro/in vivo

We examined PAR2 expression in HepG2 cells exposed to PAR2-siRNA. PAR2 knockdown was induced 24 h after PAR2-siRNA treatment at 25 nM. To further illustrate the importance of FoxO6 in inflammation, we used a siRNA-mediated gene approach to knock down FoxO6 expression in HepG2 cells, which was performed by treating the cells with PAR2-siRNA. Levels of AP-1 gene expression increased with FoxO6 expression but were reduced when cells were treated with PAR2-siRNA (Fig. 5A). We examined the ability of FoxO6 to stimulate pro-inflammatory AP-1 expression in HepG2 cells. FoxO6 activates MAPKs and AP-1. We found that FoxO6-mediated induction of IL-1β, PAR2,

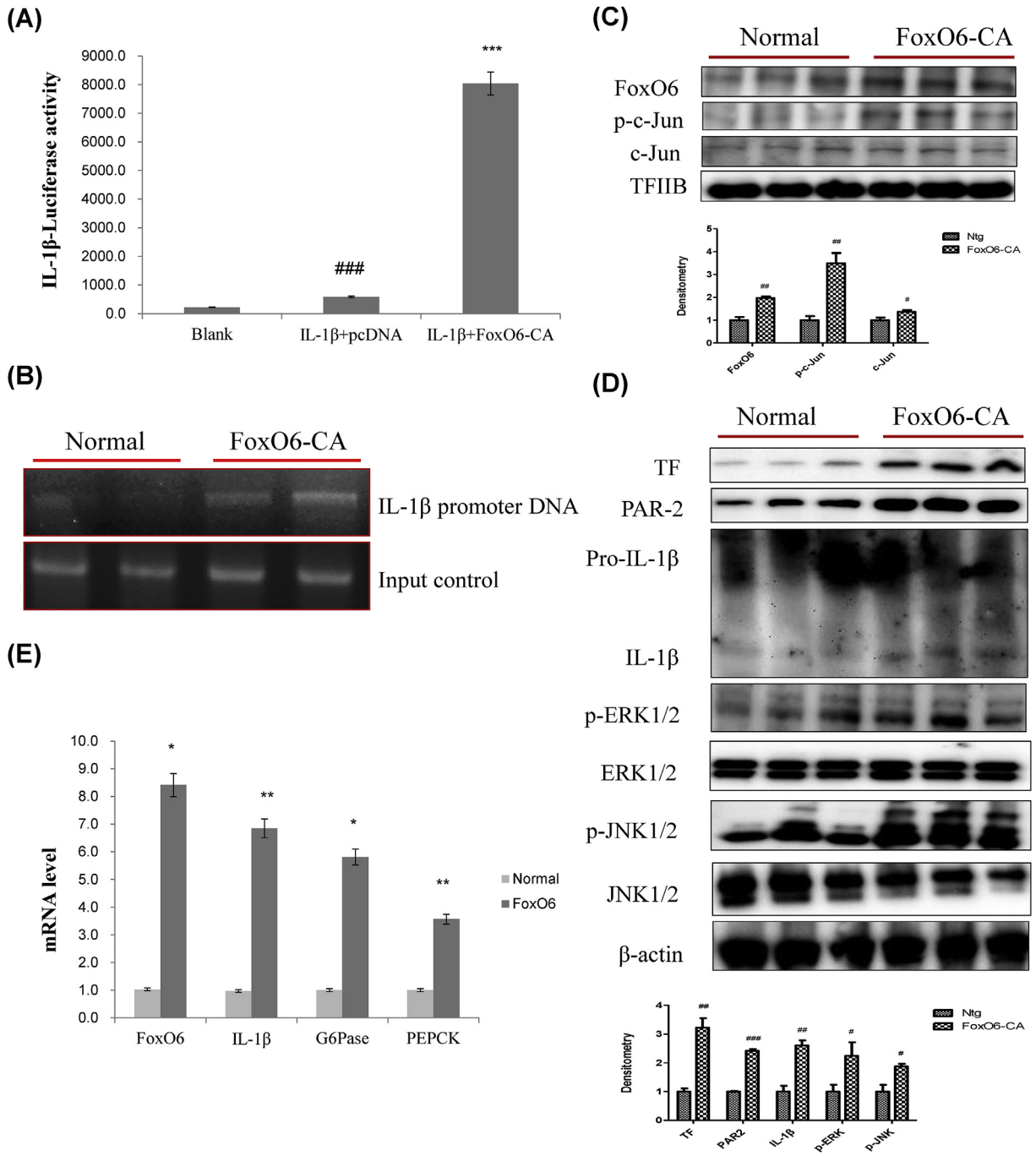

Fig. 4. FoxO6-induced IL-1β regulates insulin signaling and inflammation. (A) Effect of wild-type FoxO6 on the activity of the IL-1β promoter. HepG2 cells in 48-well microplates were transduced with AdV-FoxO6, or control AdV-null vectors at a fixed dose (MOI, 100 pfu/cell), followed by transfection with 0.5 μg of pCDNA in the culture medium. Results are presented in relative luminescence units (RLU). Results were obtained using one-factor ANOVA: $^{###}p < 0.001$ vs. blank; $^{***}p < 0.001$ vs. IL-1β treated cells. (B) FoxO6 bound to the IL-1β promoter in HepG2 cells transfected with the FoxO6 vector (100 MOI). After incubation for 24 h, the cells were subjected to a chromatin immunoprecipitation (ChIP) assay using rabbit pre-immune IgG (lanes 1, 2), or anti-FoxO6 antibody (lanes 3, 4). The immunoprecipitates were subjected to PCR using the IL-1β promoter. (C) Western blot was used to detect FoxO6, p-c-Jun, c-Jun in liver nuclei; TFIIB levels were used as loading controls. Bars in densitometry data represent means ± SE, and significance was determined using an unpaired *t*-test: $^{#}p < 0.05$, $^{##}p < 0.01$ vs. Ntg. (D) Western blot was used to detect TF, PAR2, IL-1β, p-ERK, ERK, p-JNK1/2, and JNK1/2 in liver tissues; β-actin levels were used as loading controls. Bars in densitometry data represent means ± SE, and significance was determined using an unpaired *t*-test: $^{#}p < 0.05$, $^{##}p < 0.01$, $^{###}p < 0.001$ vs. Ntg. (E) The expression of relevant genes (FoxO6, IL-1β, G6Pase, and PEPCK) was analyzed by qPCR. The results were normalized with respect to actin levels. $^{*}p < 0.05$, $^{**}p < 0.01$ vs. Normal.

and p-ERK was reduced by treatment with PAR2-siRNA. However, FoxO6 treatment also increased serine phosphorylation of insulin receptor substrate-1 (IRS-1) and thus increased tyrosine phosphorylation of IRS-1 and phosphorylation of JNK. These effects were reversed in cells treated with PAR2-siRNA (Fig. 5B). To determine whether PAR2 plays a role in linking insulin resistance to aberrant cytokine expression *in vivo*, we studied insulin signaling and cytokine expression in PAR2-KO mice. PAR2, FoxO6, AP-1, and JNK signaling were suppressed in PAR2-KO mice. However, IRS/Akt signaling increased in the PAR2-KO liver (Fig. 5C).

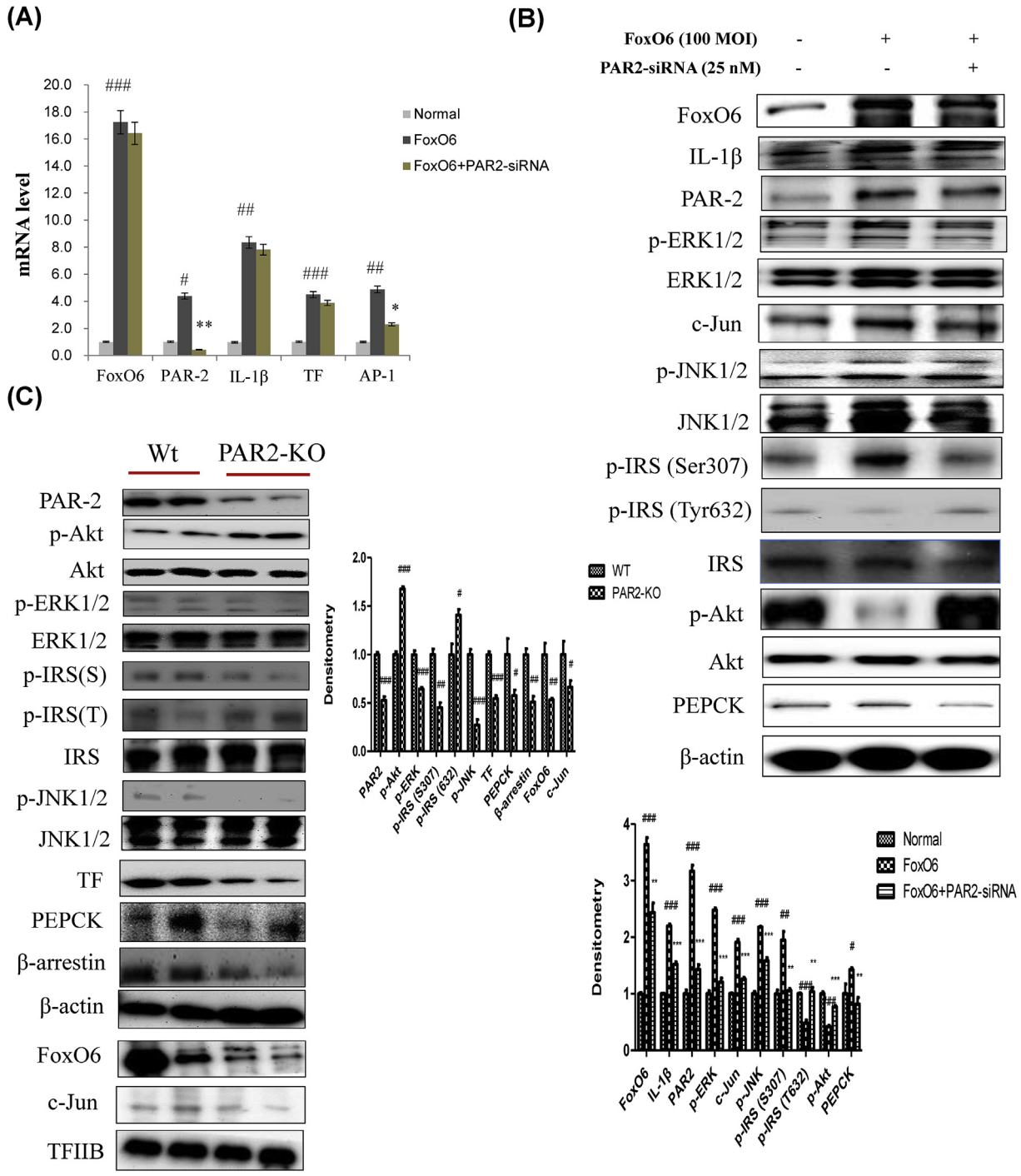

Fig. 5. FoxO6 induced inflammation through PAR2 in HepG2 cells and PAR2-KO mice. (A) Cells transfected with the FoxO6 vector (100 MOI), pre-incubated with PAR2-siRNA (25 nM) for 24 h were subjected to qRT-PCR analysis using actin as a control. FoxO6, PAR2, IL-1β, TF, and AP-1 mRNA levels were assessed. The results were normalized with respect to actin levels. $^{\#}p < 0.05$, $^{\#\#}p < 0.01$, $^{\#\#\#}p < 0.001$ vs. Normal; $^{*}p < 0.05$, $^{**}p < 0.01$ vs. FoxO6 treated group. (B) HepG2 cells were transiently transfected pre-incubated with PAR2-siRNA (25 nM) for 24 h with or without FoxO6 (100 MOI). Cells were analyzed by Western blotting using FoxO6, IL-1β, PAR2, p-ERK1/2, ERK1/2, AP-1 (c-Jun), PEPCK, p-JNK1/2, JNK1/2, p-IRS (S307), p-IRS (T632), IRS, p-Akt, Akt, and β-actin antibodies. Bars in densitometry data represent means ± SE, and significance was determined using an unpaired *t*-test: $^{\#}p < 0.05$, $^{\#\#}p < 0.01$, $^{\#\#\#}p < 0.001$ vs. Normal; $^{**}p < 0.01$, $^{***}p < 0.001$ vs. FoxO6 treated cells. (C) FoxO6, p-c-Jun, c-Jun, PAR2, p-IRS (S307), p-IRS (T632), IRS, p-Akt, Akt, p-JNK1/2, and JNK1/2 levels were assessed using nuclear and cytosolic proteins isolated from the liver samples of PAR2-KO mice. TFIIB was the loading control of the nuclear fraction. β-actin was the loading control of the cytosolic fractions. Results are representative of three independent experiments. Bars in densitometry data represent means (n = 4) ± SE, and significance was determined using an unpaired *t*-test: $^{\#}p < 0.05$, $^{\#\#}p < 0.01$, $^{\#\#\#}p < 0.001$ vs. wt.

3.6. IL-1β induces insulin resistance via the PAR2 pathway in HepG2 cells

We examined PAR2 expression in HepG2 cells exposed to IL-1β. Cells were treated with or without different concentrations (1–50 ng/ml of IL-1β). Treatment with IL-1β at 10 ng/ml induced PAR2 expression (Supplementary Fig. 4). To further illustrate the importance of cytokine IL-1β, we used the siRNA-mediated gene approach to knock down PAR2 expression in HepG2 cells, by treating the cells with PAR2-siRNA

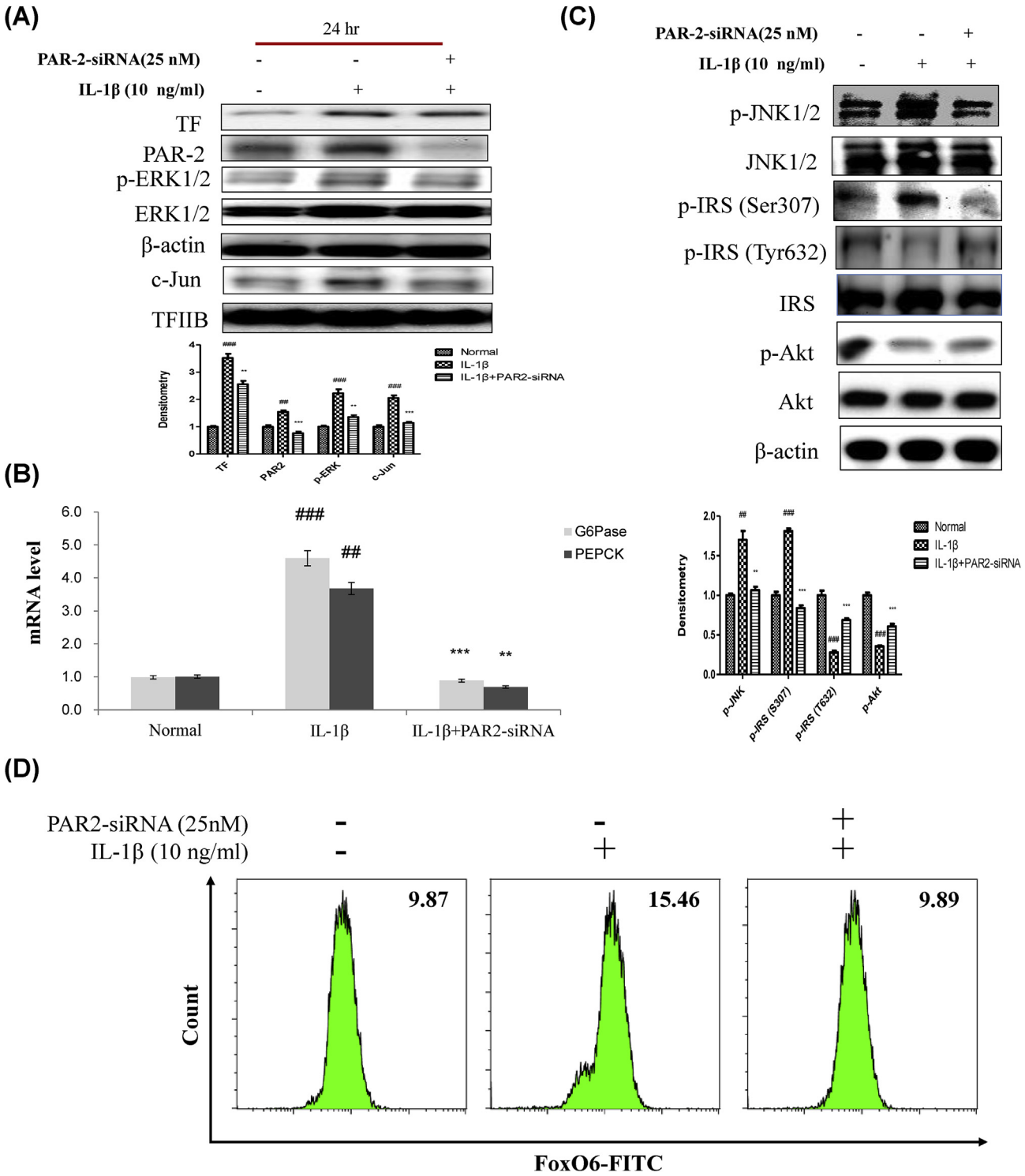

Fig. 6. IL-1β induced insulin resistance *via* the PAR2 pathway. (A) HepG2 cells were grown to 80% confluence in 100-mm dishes in DMEM medium, pre-treated (1 day) with or without PAR2-siRNA (25 nM), and then stimulated with IL-1β (10 ng/ml) and analyzed by Western blotting using antibodies. Bars in densitometry data represent means ± SE, and significance was determined using an unpaired *t*-test: $^{\#\#}p < 0.01$, $^{\#\#\#}p < 0.001$ vs. Normal; $^{**}p < 0.01$, $^{***}p < 0.001$ vs. IL-1β treated cells. (B) Gluconeogenesis genes (G6P and PEPCK) were subjected to real-time qRT-PCR analysis. Results of one factor ANOVA: $^{\#\#}p < 0.01$, $^{\#\#\#}p < 0.001$ vs. Normal; $^{**}p < 0.01$, $^{***}p < 0.001$ vs. IL-1β-treated group. (C) HepG2 cells were transiently transfected pre-incubated with PAR2-siRNA (25 nM) for 24 h with or without IL-1β (10 ng/ml). Cells were analyzed by Western blotting using p-JNK1/2, JNK1/2, p-IRS (S307), p-IRS (T632), IRS, p-Akt, and Akt antibodies. Bars in densitometry data represent means ± SE, and significance was determined using an unpaired *t*-test: $^{\#\#}p < 0.01$, $^{\#\#\#}p < 0.001$ vs. Normal; $^{**}p < 0.01$, $^{***}p < 0.001$ vs. IL-1β treated cells. (D) HepG2 cells were transiently transfected with PAR2-siRNA or control siRNA for 24 h using lipofectamine 2000 and then stimulated with IL-1β (10 ng/ml) for 24 h. The cells were stained with anti-FoxO6 and FITC goat anti-Rabbit IgG.

followed by IL-1β treatment at 10 ng/ml.

As shown in Fig. 6A, IL-1β enhanced ERK phosphorylation and reduced phosphorylated ERK levels in PAR2-siRNA-treated HepG2 cells. It also reduced PAR2 and p65 levels in PAR2-siRNA transduced cells (Fig. 6A). Therefore, we examined the ability of IL-1β to stimulate gluconeogenesis-related genes, including G6Pase and PEPCK, in HepG2 cells. IL-1β-induced G6Pase and PEPCK levels were reduced by PAR2-siRNA (Fig. 6B). However, IL-1β treatment also increased serine phosphorylation of the insulin receptor substrate-1 (IRS-1) and thus decreased tyrosine phosphorylation of IRS-1. In addition, IL-1β elevated the phosphorylation of JNK, which has been known to phosphorylate the serine residue of IRS-1. Thus, we assume that IL-1β-mediated JNK phosphorylation contributes to the impaired insulin signaling in HepG2 cells. These effects were reversed in PAR2-siRNA groups treated with IL-1β (Fig. 6C). As shown in Fig. 5A and B, FoxO6-CA-induced mRNA and protein expression of IL-1β and PAR2, but PAR2-siRNA treatment did not affect the protein level of IL-1β. As shown in Fig. 6D, we also investigated whether IL-1β treatment induced FoxO6 expression in the absence or presence of PAR2. As a result, IL-1β induced FoxO6 expression, and down-regulation of PAR2 inhibited the IL-1β-mediated induction of FoxO6.

3.7. Impacts of aging on insulin resistance and cytokine production

Insulin resistance was significantly unregulated, correlating with the pathogenesis of fasting hyperglycemia in the aging process. Aberrant pro-inflammatory cytokine production is intertwined with insulin resistance in obesity and T2D. To better understand the relationship between the molecular basis of the pro-inflammatory cytokine production and insulin resistance, we determined the relationship between insulin resistance and hepatic cytokine production using 6- and 24-month-old male Fischer 344 rats. As shown in Fig. 7, hyperinsulinemia developed with aging, culminating in significantly elevated fasting glucose (Fig. 7A) and insulin levels (Fig. 7B), as opposed to age/sex-matched control littermates. However, aging resulted in a significant increase in IL-1β and IL-6 production, without alterations in the production of other cytokines such as TNFα, leading to age-related inflammation. These data showed the importance of aging in regulating cytokine production and inflammation *in vivo* (Fig. 7C–E).

Aging was accompanied by increased expression of PEPCK and G6Pase, two key genes in gluconeogenesis (Fig. 7F). Hepatic CXCL5, IL-6, MCP-1, and IL-1β mRNA levels were also increased in aging (Fig. 7G). No difference was found in TNFα mRNA levels in old compared with the young liver. These data indicated the importance of aging in regulating cytokine production *in vivo*. To identify the cells in which inflammation markers accumulated, liver sections were stained with an antibody against CD-68. Immunofluorescence assays showed that the macrophage marker CD-68 localized to the liver (Fig. 7H), indicating that inflammation is activated in the liver *via* macrophage recruitment.

To determine whether aging plays a role in linking inflammation to aberrant IL-1β expression, we studied the expression of genes related to inflammation and IL-1β in the aging liver. Aging was accompanied by increased expression of TF and PAR2 mRNA (Fig. 7I). However, hepatic PAR2, JNK, AP-1, and FoxO6 levels were also increased in the aging group (Fig. 7J). We measured the relationship of IRS/Akt pathway to insulin resistance signaling. This result showed that phosphorylated-IRS and phosphorylated-Akt levels increased in aging (Fig. 7K) compared with young groups. Levels of COX-2 and iNOS mRNA, two key enzymes in inflammation, were increased compared with the aging group (Fig. 7L).

3.8. Inflammation and insulin resistance are induced through TF/PAR2 signaling in T2D

To determine whether a role in linking the insulin resistance to aberrant cytokine expression, we studied insulin resistance and cytokine expression in db/db mice. Insulin resistance models showed significantly increased expression of FoxO6, TF, and PAR2. Also, T2D was accompanied by increased expression of PEPCK and G6Pase, two key genes in gluconeogenesis. However, this effect was accompanied by increased expression of TNFα, IL-6, IL-1β, and MCP-1 (Fig. 8A) in db/db. We also investigated TF/PAR2 and insulin signaling by western blotting. TF, PAR2, FoxO6, AP-1, and JNK signaling were increased in db/db (Fig. 8B). Furthermore, IRS/Akt signaling was suppressed in the db/db liver (Fig. 8C).

4. Discussion

In the present study, we show evidence that the FoxO6 transcription factor independently mediates hepatic inflammation and insulin resistance through PAR2 expression. The merit and significance of our investigation is the identification of cross-talk between FoxO6 and PAR2. To date, little is known about the regulation of PAR2 by FoxO6. Here, we were able to show that liver IL-1β expression is regulated by FoxO6, a key nuclear transcription factor that mediates TF and PAR2 expression as depicted in Fig. 4. Furthermore, we validated that insulin resistance and inflammation are suppressed in PAR2-KO mice as shown in Fig. 5, revealing the crucial role of TF/PAR2 signaling in hepatic metabolic abnormalities associated with aging and obesity.

PAR2 activation in adipose macrophages induces M1 polarization and increases proinflammatory mediators [7]. However, many proteases signal through PAR2, and the role of PAR2 activation by each protease in inflammation, metabolism, and obesity remain poorly understood. Previously reported PAR2 antagonists are not selective, potent, bioavailable, or effective against protease-activated PAR2, and thus, have not been used for inhibiting PAR2-mediated disease [18,19]. However, PAR2 activation in macrophages and adipocytes suppresses Akt signaling, as well as the expression of downstream metabolic genes, resulting in insulin resistance and obesity [20].

Lim et al. [21] reported that palmitic and other fatty acids can upregulate the expression of PAR2 mRNA, and augment PAR2-activated secretion of the proinflammatory cytokines IL-1β and IL-6 in HMDMs, supporting that PAR2 is an important regulator of metabolic homeostasis and inflammatory pathways. However, Su et al. [4] reported on the molecular basis of the link between insulin resistance and induction of pro-inflammatory cytokines. It follows that in insulin-resistant states, loss of insulin inhibition by FoxO1 activity consequently results in unrestrained IL-1β expression in activated macrophages.

In addition, FoxO6 establishes an association between abnormal production of the pro-inflammatory cytokine IL-1β and the pathogenesis of insulin resistance through the PAR2 pathway in liver cells. Furthermore, hematopoietic TF/PAR2 signaling plays a pivotal role in the hepatic inflammatory response and insulin resistance that consequently lead to systemic insulin resistance and T2D in obesity [22]. Obesity and aging are multifaceted disorders involving complex cross-talk between metabolic and immune systems. These systems involve proteases that contribute to nutrient sensing, protein degradation, and metabolism, recruitment of immune cells to sites of inflammatory and metabolic stress, and damaged cells [23]. These observations suggest that TF/PAR2 signaling plays a role in hepatic inflammation and insulin resistance in gain- and loss-FoxO6 mice.

On the other hand, our data show that PAR2 knockdown ameliorated inflammation by inhibiting the ERK and JNK pathways in the liver by reducing macrophage infiltration and ameliorating insulin resistance (Fig. 6). However, PAR2 induced inflammation *via* the ERK/JNK pathway in aging models (Fig. 7). Among the various roles of MAPKs, ERK and JNK are reported to be involved in proliferation [24] and inflammation [25] of endothelial cells. In the downstream signaling pathway of ERK and JNK, some subunits of AP-1 are activated in response to ERK and JNK, and these include c-Fos, c-Jun, ATF, and JDP. The ERK and JNK pathways (with the involvement of AP-1) play an

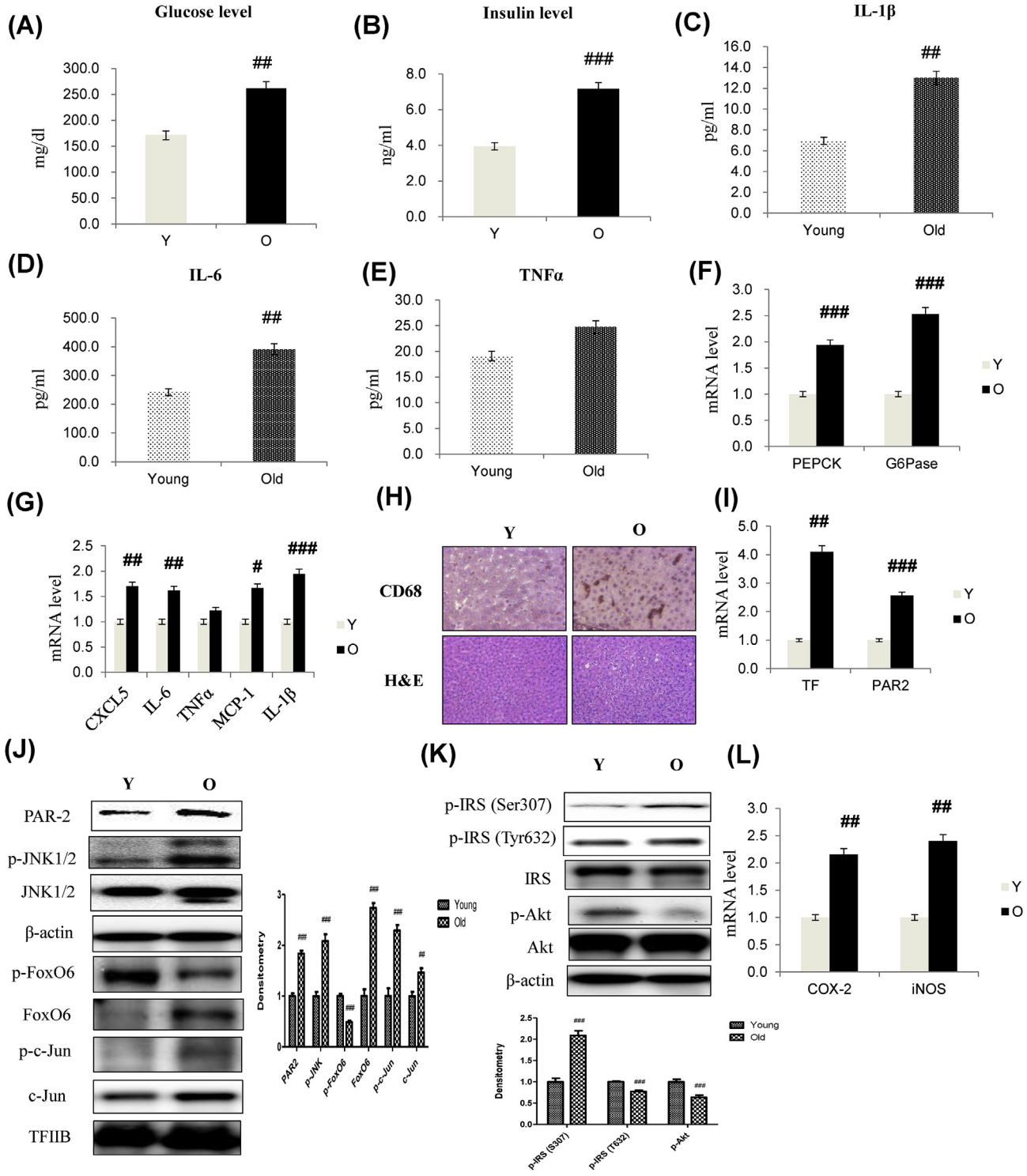

Fig. 7. Aging-induced insulin resistance and expression of pro-inflammatory genes through TF/PAR2 signaling. To test the relationship among aging, insulin resistance, and the expression of pro-inflammatory genes, 6- and 24-month-old male Fischer 344 rats were used. (A) Glucose level (B) Insulin level in serum of aged models. Cytokine levels of (C) IL-1β (D) IL-6 (E) TNFα in serum using ELISA assay. The results shown are representative of three experiments. The data are expressed as a mean ± SEM (n = 6). $^{\#\#}p < 0.01$, $^{\#\#\#}p < 0.001$ vs. Young. (F) G6Pase and PEPCK mRNA (G) CXCL5, IL-6, TNFα, MCP-1, and IL-1β mRNA. Real-time PCR analyses were performed to determine mRNA levels in liver tissues of young (6 months) and old (24 months) rats. The results shown are representative of three experiments. $^{\#}p < 0.05$, $^{\#\#}p < 0.01$, $^{\#\#\#}p < 0.001$ vs. Young. (H) Representative macrophage recruitment immunohistochemistry. Liver sections were stained with a specific antibody against the macrophage marker, CD68. (I) mRNA levels of TF and PAR2 genes. $^{\#\#}p < 0.01$, $^{\#\#\#}p < 0.001$ vs. Young. Western blot analyses of liver nuclear and cytosolic (J) PAR2, p-JNK1/2, JNK1/2, p-FoxO6, FoxO6, p-c-Jun, c-Jun (K) p-IRS1 (S307), p-IRS (T632), IRS, p-Akt, and total-Akt levels were performed using nuclear and cytosolic proteins from aged rats. Results are representative of three independent experiments. TFIIB was the loading control of the nuclear fraction. β-actin was the loading control of the cytosolic fractions. Bars in densitometry data represent means ± SE, and significance was determined using an unpaired *t*-test: $^{\#\#}p < 0.01$, $^{\#\#\#}p < 0.001$ vs. Young. (L) COX-2 and iNOS mRNA levels of pro-inflammatory genes. The data are expressed as the mean ± SEM. $^{\#\#}p < 0.01$ vs. Young.

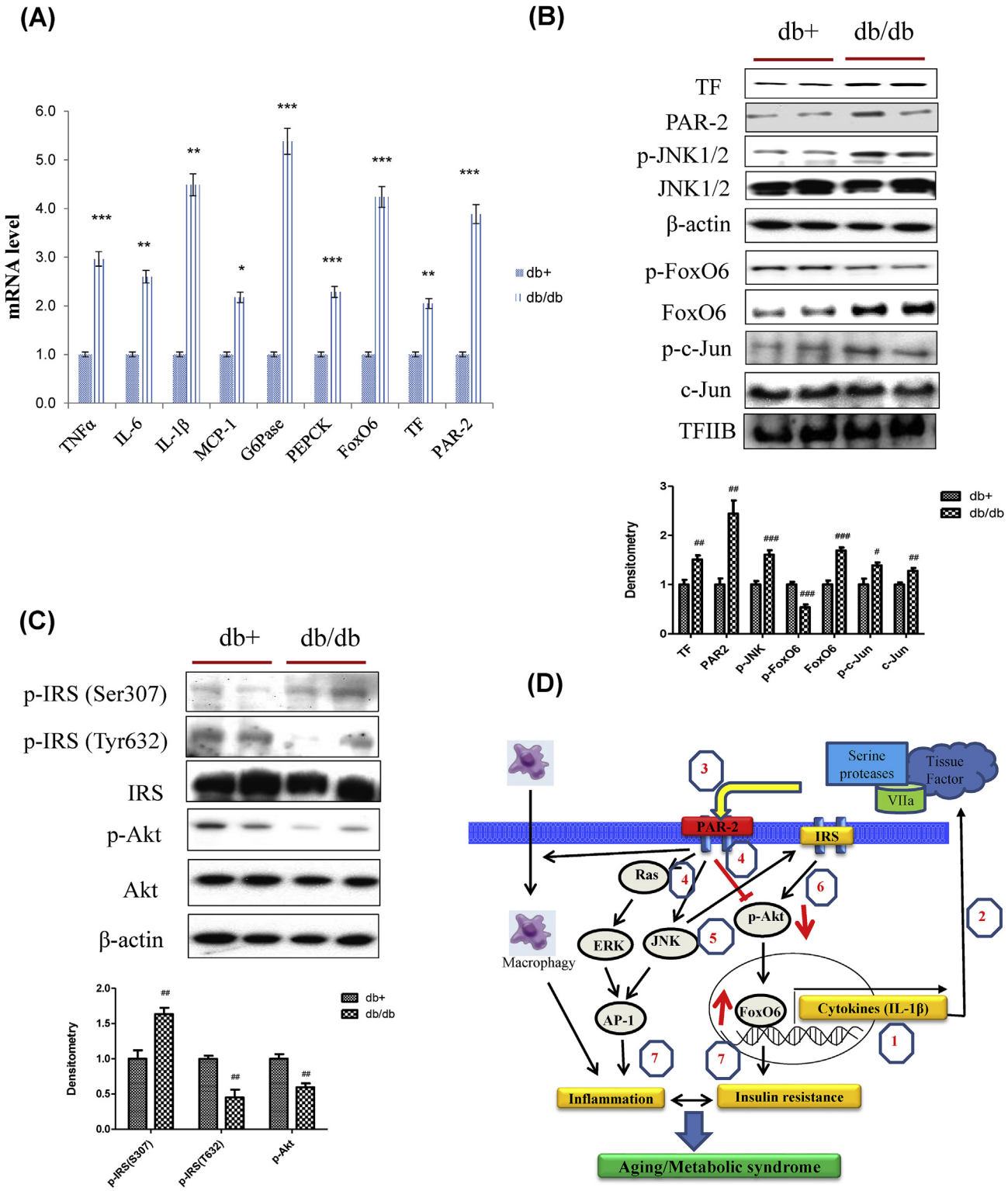

Fig. 8. Obesity-induced inflammation and insulin resistance through TF/PAR2 signaling. (A) TNFα, IL-6, IL-1β, MCP-1, G6Pase, PEPCK, FoxO6, TF, and PAR2 mRNA. Real-time PCR analyses were performed to determine mRNA levels in liver tissues of db/db mice (n = 4 in each group). The results shown are representative of three experiments. $^{*}p < 0.05$, $^{**}p < 0.01$, $^{***}p < 0.001$ vs. db+. (B) TF, PAR2, p-JNK1/2, JNK1/2, p-FoxO6, FoxO6, p-c-Jun, and c-Jun levels were assessed using nuclear and cytosolic proteins from db/db mice. TFIIB was the loading control of the nuclear fraction. β-actin was the loading control of the cytosolic fractions. Results are representative of three independent experiments. Bars in densitometry data represent means ± SE, and significance was determined using an unpaired *t*-test: $^{\#}p < 0.05$, $^{\#\#}p < 0.01$, $^{\#\#\#}p < 0.001$ vs. db^{+}. (C) p-IRS (S307), p-IRS (T632), IRS, p-Akt, and total-Akt levels were assessed using cytosolic proteins from db/db mice. β-actin was the loading control of the cytosolic fractions. Results are representative of three independent experiments. Bars in densitometry data represent means ± SE, and significance was determined using an unpaired *t*-test: $^{\#\#}p < 0.01$ vs. db^{+}. (D) A possible mechanism underlying the effect of FoxO6 on PAR2 signaling in aging. PAR2, protease-activated receptor 2; FoxO6, Forkhead transcription factor O6. Figure out: 1, FoxO6 induced IL-1β; 2, secreted IL-1β mediated tissue factor; 3, Tissue factor activated PAR2; 4, PAR2 induced ERK and JNK, and inhibited Akt level; 5, JNK induced phosphorylation of Ser-IRS; 6, Phosphorylated IRS inhibited Akt; 7, Activated ERK and JNK induced inflammation by AP-1, dephosphorylation of Akt mediated insulin resistance through FoxO6 activation. However, activation of FoxO6 induced IL-1β again.

essential role in pro-inflammatory cytokine production [26], and induction of enzymes such as COX-2 [27]. Hepatic inflammation induced by local immune cells is linked to pathways that lead to hepatic insulin resistance in response to obesity [28,29]. The link between insulin resistance and an inflammatory pathological state in the obese liver further induces and recruits macrophage cells [22]. To date, neither the inflammatory response in the obese liver with respect to macrophages and other immune cells nor the signaling pathways that activate pro-inflammatory responses are well characterized.

We previously reported [30] that aged rats showed higher insulin resistance and IL-1β levels in the liver than young rats, and in the present study, we further examined the TF/PAR2 response in diabetic mice and aged rats. We found that the increase in PAR2 levels in response to FoxO6 was greater in obese and aged rat livers and that inflammation and FoxO6-induced increases in IL-1β levels were higher in obese and aged rat livers. These results are important because PAR2 is involved in the upregulation of inflammation and insulin resistance. These observations suggest that TF/PAR2-mediated insulin resistance and inflammation of the liver and hepatocytes have significant physiological and pathological roles in diabetes and aging models.

Uncontrolled gluconeogenesis is one of the hallmarks of the liver with insulin resistance. We also found that the highly increased mRNA levels of PEPCK and G6Pase in the liver samples of old rats and obese mice that exhibited hepatic insulin resistance (Figs. 7I and 8A). However, it is not fully understood how these gluconeogenesis genes are regulated under the insulin resistant condition. Our study showed that FoxO6/IL-1β/PAR2 axis may be involved in this process. In both old rats and obese mice, the protein levels of FoxO6 and PAR2 were elevated with the increase in the mRNA levels of IL-1β in the liver. In vitro studies using HepG2 cells indicate that FoxO6 is able to bind to the promoter of IL-1β and stimulate its transcription (Fig. 4A, B, and E). Furthermore, IL-1β treatment elevated the protein levels of PAR2 with the significant increase in the mRNA levels of G6Pase and PEPCK, whereas PAR2-siRNA treatment abolished the IL-1β-mediated upregulation of gluconeogenesis genes (Fig. 6A and B). However, PAR2-siRNA treatment had no effect on the mRNA and protein levels of IL-1β induced by FoxO6, indicating that IL-1β may not be downstream of PAR2. Based on these data, we think that the FoxO6-mediated IL-1β induction is important for PAR2 activation followed by the induction of gluconeogenesis genes in insulin-resistant state. The present study aimed to elucidate the mechanisms underlying the role of FoxO6 in TF/PAR2 signaling under potent pro-inflammatory conditions induced by IL-1β, leading to insulin resistance (Fig. 8D). Furthermore, we present evidence showing that TF/PAR2-mediated inflammation and insulin resistance in aging and obesity is derived from activation of the pro-inflammatory transcription factor AP-1 *via* the ERK and JNK pathways in the FoxO6-KO and PAR2-KO mouse liver, and HepG2 cells.

In conclusion, this study delineated that FoxO6-induced IL-1β plays a pivotal role in the inflammatory response and hepatic insulin resistance by inducing infiltration of macrophages *via* activation of the TF/PAR2 pathway in murine models of type 2 diabetes and aging. A better understanding of the novel mechanism of PAR2 in diabetes and aging should promote the further development of therapeutic interventions against diabetes and aging.

Conflicts of interest

The authors have no potential conflicts of interest to declare.

Acknowledgments

This work was supported by a National Research Foundation (NRF) grant funded by the Korean government (MSIT-2018R1A2A3075425; MSIP-2009-0083538). In addition, this research was supported by the Basic Science Research Program through the National Research Foundation of Korea (NRF) funded by the Ministry of Education (NRF-2018R1A6A3A11046180). We also take this opportunity to thank the Aging Tissue Bank (Busan, Korea) for supplying aged tissue.

Appendix A. Supplementary data

Supplementary data to this article can be found online at https://doi.org/10.1016/j.redox.2019.101184.

References

[1] D. Accili, K.C. Arden, FoxOs at the crossroads of cellular metabolism, differentiation, and transformation, Cell 117 (2004) 421–426.
[2] S. Karger, C. Weidinger, K. Krause, S.Y. Sheu, T. Aigner, O. Gimm, K.W. Schmid, H. Dralle, D. Fuhrer, FOXO3a: a novel player in thyroid carcinogenesis? Endocr. Relat. Cancer 16 (2009) 189–199.
[3] L.P. Van der Heide, M.F.M. Hoekman, M.P. Smidt, The ins and outs of FoxO shuttling: mechanisms of FoxO translocation and transcriptional regulation, Biochem. J. 380 (2004) 297–309.
[4] D. Su, G.M. Coudriet, D.H. Kim, Y. Lu, G. Perdomo, S. Qu, S. Slusher, H.M. Tse, J. Piganelli, N. Giannoukakis, J. Zhang, H.H. Dong, FoxO1 links insulin resistance to proinflammatory cytokine IL-1beta production in macrophages, Diabetes 58 (2009) 2624–2633.
[5] S. Affo, O. Morales-Ibanez, D. Rodrigo-Torres, J. Altamirano, D. Blaya, D.H. Dapito, C. Millán, M. Coll, J.M. Caviglia, V. Arroyo, J. Caballería, R.F. Schwabe, P. Ginès, R. Bataller, P. Sancho-Bru, CCL20 mediates lipopolysaccharide induced liver injury and is a potential driver of inflammation and fibrosis in alcoholic hepatitis, Gut 63 (2014) 1782–1792.
[6] A.S. Rothmeier, W. Ruf, Protease-activated receptor 2 signaling in inflammation, Semin. Immunopathol. 34 (2012) 133–149.
[7] L. Badeanlou, C. Furlan-Freguia, G. Yang, W. Ruf, F. Samad, Tissue factor-protease-activated receptor 2 signaling promotes diet-induced obesity and adipose inflammation, Nat. Med. 17 (2011) 1490–1497.
[8] R. Srinivasan, E. Ozhegov, Y.W. van den Berg, B.J. Aronow, R.S. Franco, M.B. Palascak, J.T. Fallon, W. Ruf, H.H. Versteeg, V.Y. Bogdanov, Splice variants of tissue factor promote monocyte-endothelial interactions by triggering the expression of cell adhesion molecules via integrin-mediated signaling, J. Thromb. Haemost. 9 (2011) 2087–2096.
[9] U. Johansson, C. Lawson, M. Dabare, D. Syndercombe-Court, A.C. Newland, G.L. Howells, M.G. Macey, Human peripheral blood monocytes express protease receptor-2 and respond to receptor activation by production of IL-6, IL-8 and IL-1{beta}, J. Leukoc. Biol. 78 (2005) 967–975.
[10] V. Knight, J. Tchongue, D. Lourensz, P. Tipping, W. Sievert, Protease-activated receptor 2 promotes experimental liver fibrosis in mice and activates human hepatic stellate cells, Hepatology 55 (2012) 879–887.
[11] H.Y. Chung, B. Sung, K.J. Jung, Y. Zou, B.P. Yu, The molecular inflammatory process in aging, Antioxidants Redox Signal. 8 (2006) 572–581.
[12] M.H. Park, D.H. Kim, E.K. Lee, N.D. Kim, D.S. Im, J. Lee, B.P. Yu, H.Y. Chung, Age-related inflammation and insulin resistance: a review of their intricate interdependency, Arch. Pharm. Res. 37 (2014) 1507–1514.
[13] E. Jung, J.A. Lee, S. Shin, K.B. Roh, J.H. Kim, D. Park, Madecassoside inhibits melanin synthesis by blocking ultraviolet-induced inflammation, Molecules 18 (2013) 15724–15736.
[14] K. Maruyama, S. Kagota, J.J. McGuire, H. Wakuda, N. Yoshikawa, K. Nakamura, K. Shinozuka, Age-related changes to vascular protease-activated receptor 2 in metabolic syndrome: a relationship between oxidative stress, receptor expression, and endothelium-dependent vasodilation, Can. J. Physiol. Pharmacol. 95 (2017) 356–364.
[15] M. Bartneck, V. Fech, J. Ehling, O. Govaere, K.T. Warzecha, K. Hittatiya, M. Vucur, J. Gautheron, T. Luedde, C. Trautwein, T. Lammers, T. Roskams, W. Jahnen-Dechent, F. Tacke, Histidine-rich glycoprotein promotes macrophage activation and inflammation in chronic liver disease, Hepatology 63 (2016) 1310–1324.
[16] A.M. Shearer, R. Rana, K. Austin, J.D. Baleja, N. Nguyen, A. Bohm, L. Covic, A. Kuliopulos, Targeting liver fibrosis with a cell-penetrating PAR2 pepducin, J. Biol. Chem. 291 (2016) 23188–23198.
[17] V. Calabuig-Navarro, J. Yamauchi, S. Lee, T. Zhang, Y.Z. Liu, K. Sadlek, G.M. Coudriet, J.D. Piganelli, C.L. Jiang, R. Miller, M. Lowe, H. Harashima, H.H. Dong, Forkhead box O6 (FoxO6) depletion attenuates hepatic gluconeogenesis and protects against fat-induced glucose disorder in mice, J. Biol. Chem. 290 (2015) 15581–15594.
[18] T. Kanke, M. Kabeya, S. Kubo, S. Kondo, K. Yasuoka, J. Tagashira, H. Ishiwata, M. Saka, T. Furuyama, T. Nishiyama, T. Doi, Y. Hattori, A. Kawabata, M.R. Cunningham, R. Plevin, Novel antagonists for proteinase-activated receptor 2: inhibition of cellular and vascular responses in vitro and in vivo, Br. J. Pharmacol. 158 (2009) 361–371.
[19] E.B. Kelso, W.R. Ferrell, J.C. Lockhart, I. Elias-Jones, T. Hembrough, L. Dunning, J.A. Gracie, I.B. McInnes, Expression and proinflammatory role of proteinase activated receptor 2 in rheumatoid synovium: ex vivo studies using a novel proteinase-activated receptor 2 antagonist, Arthritis Rheum. 56 (2007) 765–771.
[20] F. Samad, W. Ruf, Inflammation, obesity, and thrombosis, Blood 122 (2013) 3415–3422.
[21] J. Lim, A. Iyer, L. Liu, J.Y. Suen, R.J. Lohman, V. Seow, M.K. Yau, L. Brown, D.P. Fairlie, Diet-induced obesity, adipose inflammation, and metabolic dysfunction correlating with PAR2 expression are attenuated by PAR2 antagonism, FASEB J. 27

(2013) 4757–4767.
[22] J. Wang, S. Chakrabarty, Q. Bui, W. Ruf, F. Samad, Hematopoietic tissue factor-protease-activated receptor 2 signaling promotes hepatic inflammation and contributes to pathways of gluconeogenesis and steatosis in obese mice, Am. J. Pathol. 18 (2015) 524–535.
[23] G.H. Caughey, Mast cell tryptases and chymases in inflammation and host defense, Immunol. Rev. 217 (2007) 141–154.
[24] Y.J. Jin, J.H. Lee, Y.M. Kim, G.T. Oh, H. Lee, Macrophage inhibitory cytokine-1 stimulates proliferation of human umbilical vein endothelial cells by up-regulating cyclins D1 and E through the PI3K/Akt-, ERK-, and JNK-dependent AP-1 and E2F activation signaling pathways, Cell. Signal. 24 (2012) 1485–1495.
[25] S.R. Kim, Y.R. Jung, D.H. Kim, H.J. An, M.K. Kim, N.D. Kim, H.Y. Chung, Caffeic acid regulates LPS-induced NF-kappaB activation through NIK/IKK and c-Src/ERK signaling pathways in endothelial cells, Arch. Pharm. Res. 37 (2014) 539–547.
[26] Y.D. Jung, F. Fan, D.J. McConkey, M.E. Jean, W. Liu, N. Reinmuth, O. Stoeltzing, S.A. Ahmad, A.A. Parikh, N. Mukaida, L.M. Ellis, Role of P38 MAPK, AP-1, and NF-kappaB in interleukin-1beta-induced IL-8 expression in human vascular smooth muscle cells, Cytokine 18 (2002) 206–213.
[27] E. Looby, M.M. Abdel-Latif, V. Athié-Morales, S. Duggan, A. Long, D. Kelleher, Deoxycholate induces COX-2 expression via Erk1/2-, p38-MAPK and AP-1-dependent mechanisms in esophageal cancer cells, BMC Canc. 9 (2009) 190.
[28] J.I. Odegaard, R.R. Ricardo-Gonzalez, A. Red Eagle, D. Vats, C.R. Morel, M.H. Goforth, V. Subramanian, L. Mukundan, A.W. Ferrante, A. Chawla, Alternative M2 activation of Kupffer cells by PPARdelta ameliorates obesity-induced insulin resistance, Cell Metabol. 7 (2008) 496–507.
[29] A.E. Obstfeld, E. Sugaru, M. Thearle, A.M. Francisco, C. Gayet, H.N. Ginsberg, E.V. Ables, A.W. Ferrante Jr., C-C chemokine receptor 2 (CCR2) regulates the hepatic recruitment of myeloid cells that promote obesity-induced hepatic steatosis, Diabetes 59 (2010) 916–925.
[30] K.W. Chung, E.K. Lee, D.H. Kim, H.J. An, N.D. Kim, D.S. Im, J. Lee, B.P. Yu, H.Y. Chung, Age-related sensitivity to endotoxin-induced liver inflammation: implication of inflammasome/IL-1β for steatohepatitis, Aging Cell 14 (2015) 524–533.